

Conversion point mapping and interpolation in P-S survey design

Don C. Lawton and Peter W. Cary

ABSTRACT

Depth-variant mapping of P-S conversion points in 3C-3D survey design shows that conversion points are distributed irregularly at the reflector, resulting in high-frequency (bin-bin) fold variations in P-S fold maps if nearest-neighbour binning is used. This binning artifact can be mitigated through the application of a sinc-function interpolator that provides a more robust measure of fold distribution for band-limited seismic data.

INTRODUCTION

At the CREWES sponsors' meeting in 1999, a paper on design issues for 3C-3D seismic data was presented (Lawton and Hoffe, 1999), in which we showed variations in asymptotic conversion point (ACP) and depth specific conversion point (DSCP) fold as a function of V_p/V_s , and as a function of water depth in the case of ocean-bottom cable (OBC) surveys. In the discussion that followed, there was debate about whether the high spatial frequency fold variations were really a serious concern, or whether they were simply an artifact of nearest-neighbour conversion point fold. This arises because in the common-shot domain, separation of conversion points is not the same as mid-point.

Subsequent to the meeting, a sinc-function interpolator was developed by Peter Cary (Cary and Lawton, 2000), and this capability was added as an option in CREWES 3C-3D design code. This paper reviews P-S fold distribution using the sinc interpolator for a simple OBC survey.

CONVERSION POINT FOLD INTERPOLATION

In nearest-neighbour interpolation, each trace is assumed to contribute to only one output bin, and therefore is essentially infinite in spatial bandwidth. Since seismic data are band-limited, the wavefields should be interpolated with a bandlimited delta function (a sinc function), so that when a P-S conversion points lies near a bin boundary, it will also contribute to the neighbouring bins. The CDP bin width determines the distance between the zero-crossings of the spatial sinc-function since this has been chosen as the spatial Nyquist sample rate at the survey design stage, and generally is a good representation of a post-stack migrated Fresnel zone for typical survey geometries. In the examples tested, an 11-point operator in both the in-line and cross-line directions was found to yield optimum results. Other interpolators may also be considered, but sinc-function interpolation is preferred over a linear interpolator, although results may be quite similar in high-fold survey designs.

EXAMPLE 1

A simple design example (Figure 1) is shown to illustrate the binning issues and interpolation discussed above. For P-S asymptotic mapping using standard P-P binning, the fold map (Figure 2) show stripes of empty bins. This occurs for situations when the source-line interval is an even integer multiple of the receiver interval and $V_p/V_s = 2$, and is due to the fact that the CCP separation in the receiver line direction is larger than the CDP separation. In Figure 2, conversion points are shown by the regular pattern of white crosses. If V_p/V_s changes slightly, for example to 2.1, there is more dispersion in CCP locations and the pattern of bin fold will change, as shown in Figure 3. A more meaningful fold distribution is obtained by using an interpolator to map fold distribution rather than the nearest-neighbour approach used in Figures 2 and 3. The results of using the sinc-function interpolator are shown in Figures 4 and 5, for asymptotic mapping and V_p/V_s of 2.0 and 2.1 respectively. The resulting fold distribution is much smoother in each display and, as one might anticipate, there is not a large difference between the fold maps resulting from only a small change in V_p/V_s .

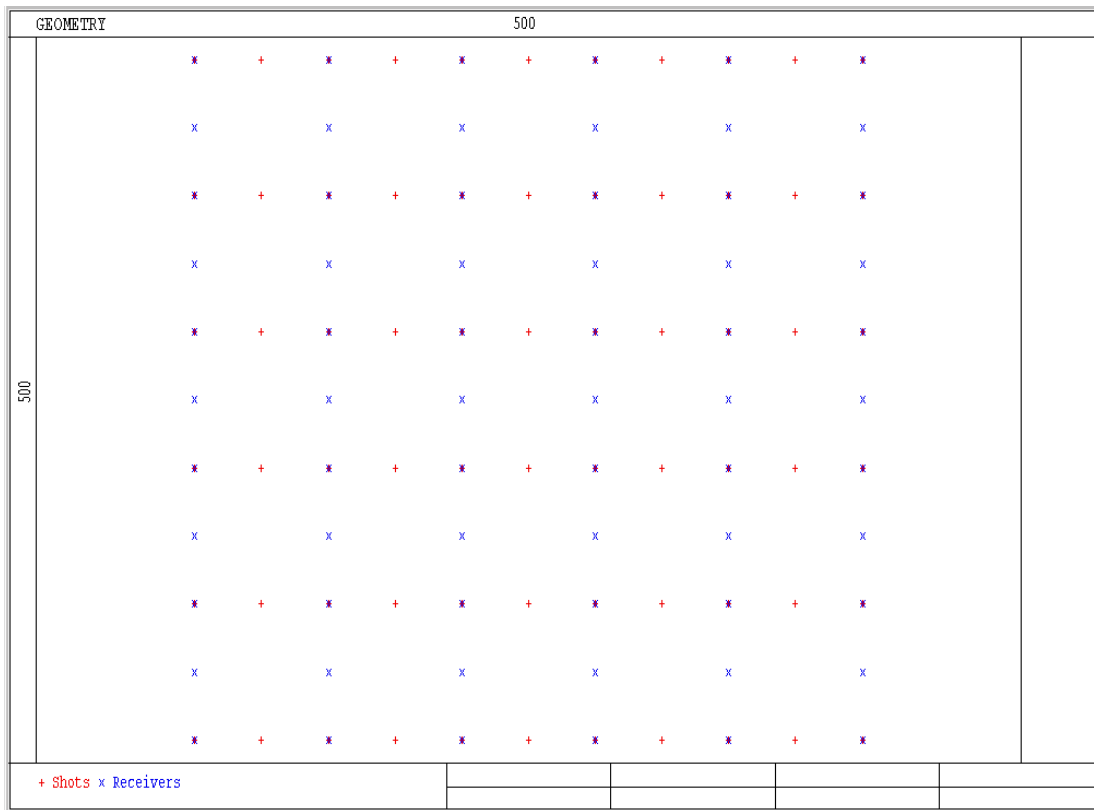


Figure 1. Orthogonal 3C-3D design, with shot and receiver line spacings of 100m, and shot and receiver separations of 50 m.

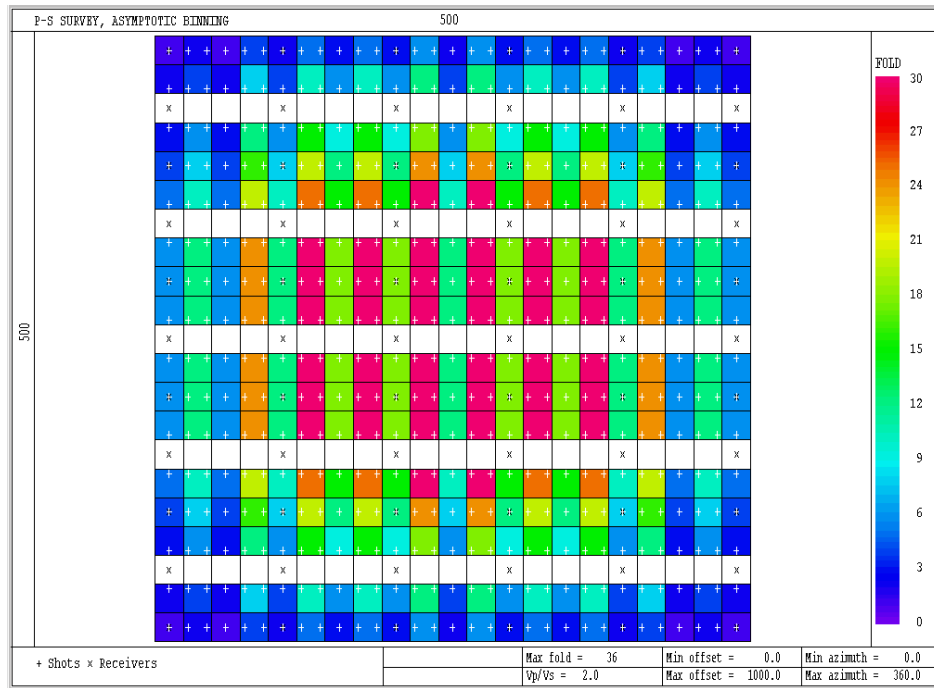


Figure 2. Asymptotic P-S fold distribution for design geometry shown in Figure 1. $V_p/V_s = 2.0$. White crosses show locations of conversion points.

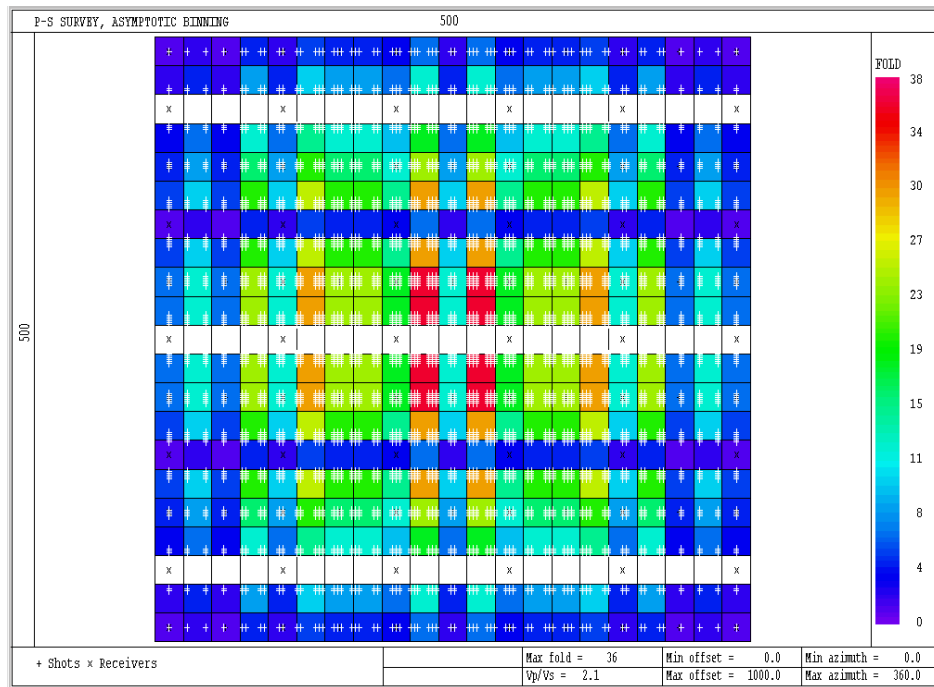


Figure 3. Asymptotic P-S fold distribution for design geometry shown in Figure 1. $V_p/V_s = 2.1$. White crosses show locations of conversion points.

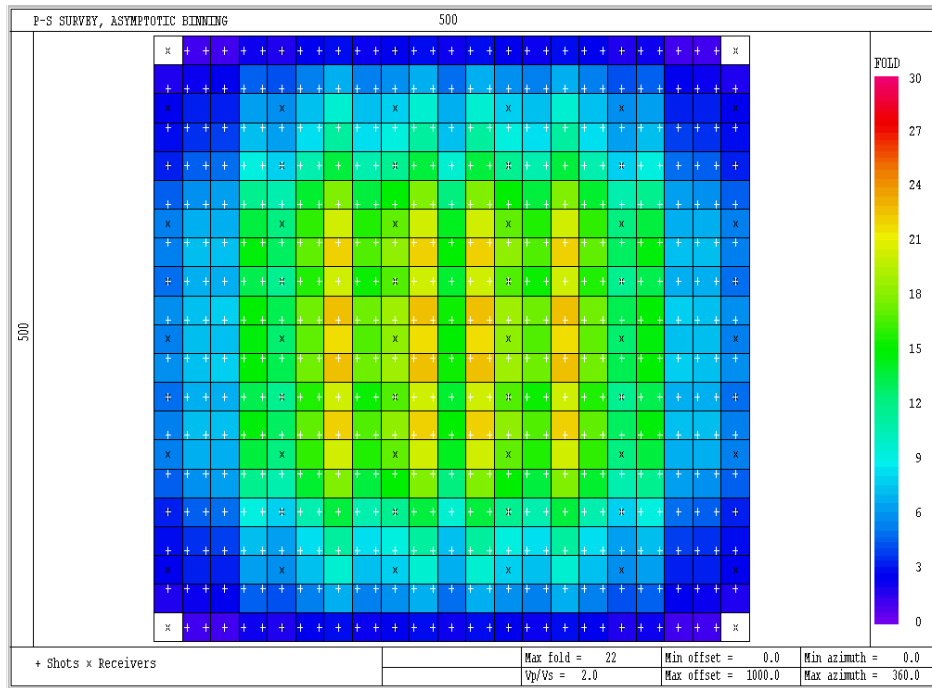


Figure 4. P-S fold distribution as shown in Figure 2 but with sinc-function interpolator applied. White crosses show locations of conversion points.

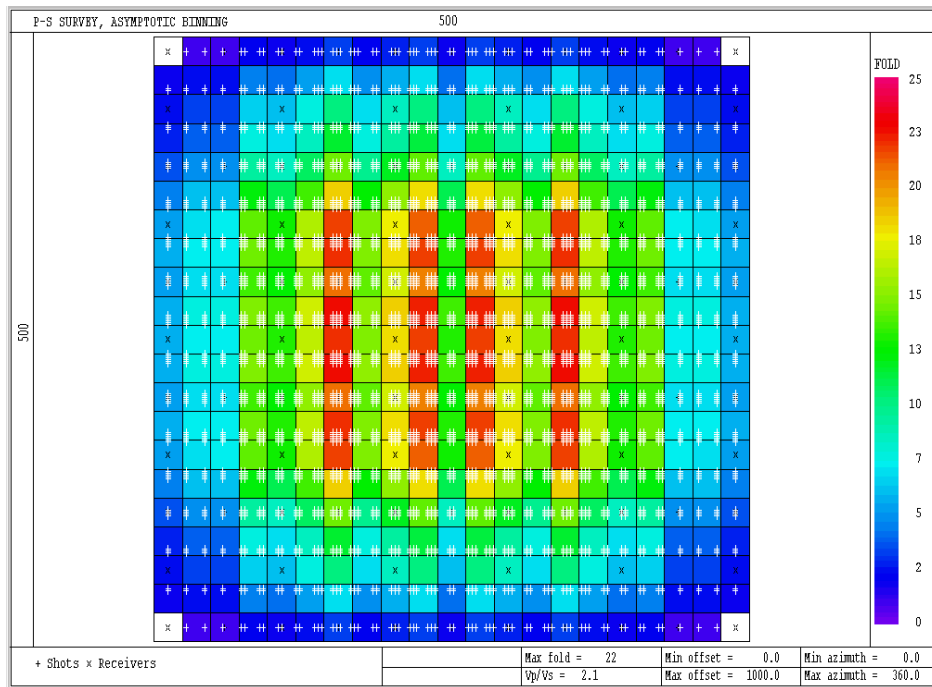


Figure 5. P-S fold distribution as shown in Figure 3 but with sinc-function interpolator applied. White crosses show locations of conversion points.

EXAMPLE 2

To examine the effect of the interpolator on a larger scale survey, a second design example is shown, based on the same geometry as illustrated by Lawton and Hoffe (1999). The survey parameters are given in Table 1, and the source and receiver geometry is shown in Figure 6.

Table 1. Source and receiver parameters for example 3C-3D OBC design.

Source Data	Parameter
Number of Source Lines	41
Source Line Separation	100 m
Number of source points/line	61
Source Interval	50 m
Source Line Orientation	0°
Total Number of Source Points	2501
Receiver Data	Parameter
Number of Receiver Lines	6
Receiver Line Separation	300 m
Number of receiver points/line	41
Receiver Interval	50 m
Receiver Line Orientation	90°
Total Number of Receiver Points	246
Bin Dimensions	25 × 25 m
Source/Receiver Effort	10.17

Figure 7 is a display of the P-S fold map for the geometry shown in Figure 6 with offsets to 2500 m, and computed using asymptotic binning for $V_p/V_s = 2.0$. This map shows stripes of empty bins parallel to the shot lines (for bin dimensions of 25 × 25 m), as predicted from criteria discussed earlier and as shown in Figure 2. If sinc-function interpolation is applied, the high spatial frequency fold variation is reduced considerably and the fold distribution is smoother, as shown in Figure 8. For DSCP mapping with a target depth of 2000m, the nearest-neighbour interpolation does not yield stripes of empty bins, but high spatial frequency fold variations persist (Figure 9) and these also are smoothed with application of the interpolator (Figure 10).



Figure 6. Source and receiver geometry for 3C-3D design example 2. Shot line spacing is 100m, receiver line spacing is 300m and shot and receiver spacings are both 50 m.

Fold variations as a function of receiver depth (OBC) and V_p/V_s

Figures 11 and 12 show DSCP P-S fold for a target depth of 2000 m and water depths of 100 m and 400 m respectively, for $V_p/V_s = 2.0$. Maximum offset is 2500 m and an 11-point sinc-function interpolator was applied. As the water depth increases, the area illuminated by this survey design decreases in size, and zones of high fold develop between the receiver lines.

Figures 13 and 14 show DSCP P-S fold for a target depth of 2000 m, a water depth of 200 m and V_p/V_s of 1.6 and 2.3 respectively. Maximum offset is 2500 m and an 11-point sinc-function interpolator was applied. As V_p/V_s increases, the area illuminated by this survey design decreases in size, but fold becomes more uniformly distributed over the receiver patch as V_p/V_s increases.

CONCLUSIONS

Assessment of fold distribution in 3C-3D surveys is improved through the use of a sinc-function interpolator that reduces high spatial frequency fold variations usually seen in P-S fold plots that are generated through nearest neighbour interpolation. The smoothed fold distributions provide a more realistic assessment of what actually occurs in the subsurface. P-S fold will vary with receiver depth (for OBC surveys) and V_p/V_s , and these should be evaluated during the design process.

REFERENCES

- Cary, P.W., and Lawton, D.C., 2000, Bandlimited survey design and CCP stacking of P-S data: SEG/EAGE Summer Research Workshop, October 1-6.
- Lawton, D.C, and Hoffe, B. H., 1999, Some design issues for 3C-3D OBC seismic data, CREWES Annual Research Report, Volume 11, 227-236.

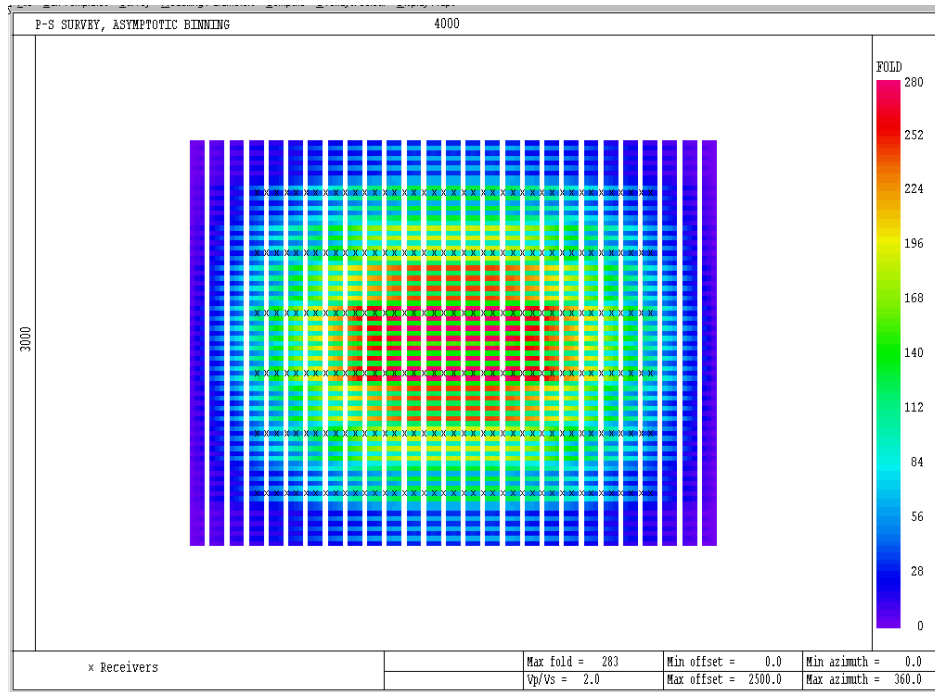


Figure 7. Asymptotic P-S fold computed for $V_p/V_s = 2.0$ and maximum offset of 2500 m. Geometry is shown in Fig. 6. No interpolation yields bins with zero fold.

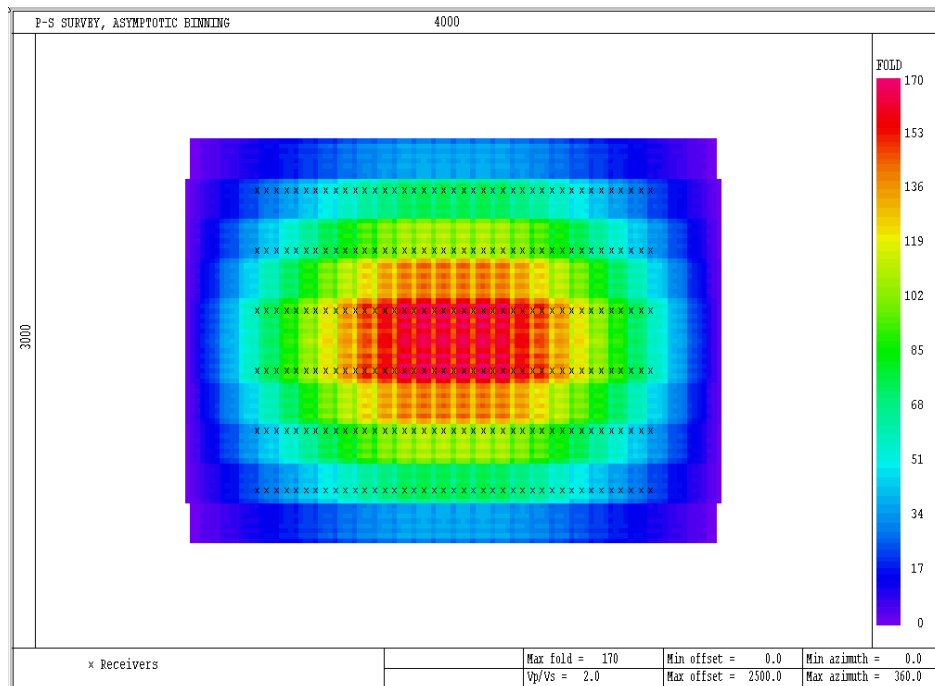


Figure 8. Asymptotic P-S fold as shown in Figure 7 but with sinc-function interpolation applied.

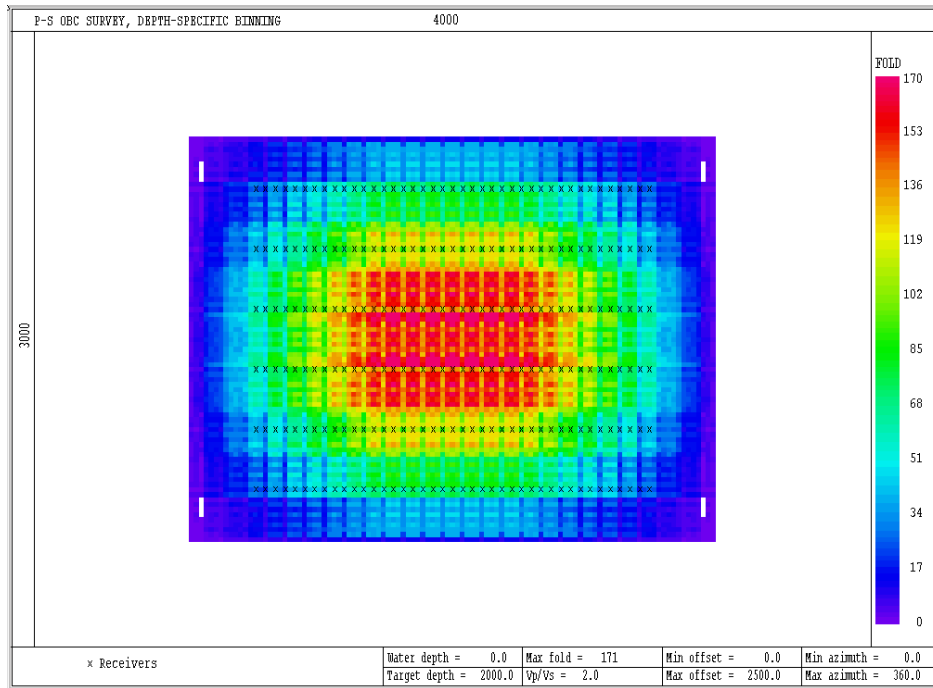


Figure 9. Depth-specific conversion point (DSCP) P-S fold for a target depth at 2000m and $V_p/V_s = 2.0$. Nearest-neighbour binning only with no interpolation.

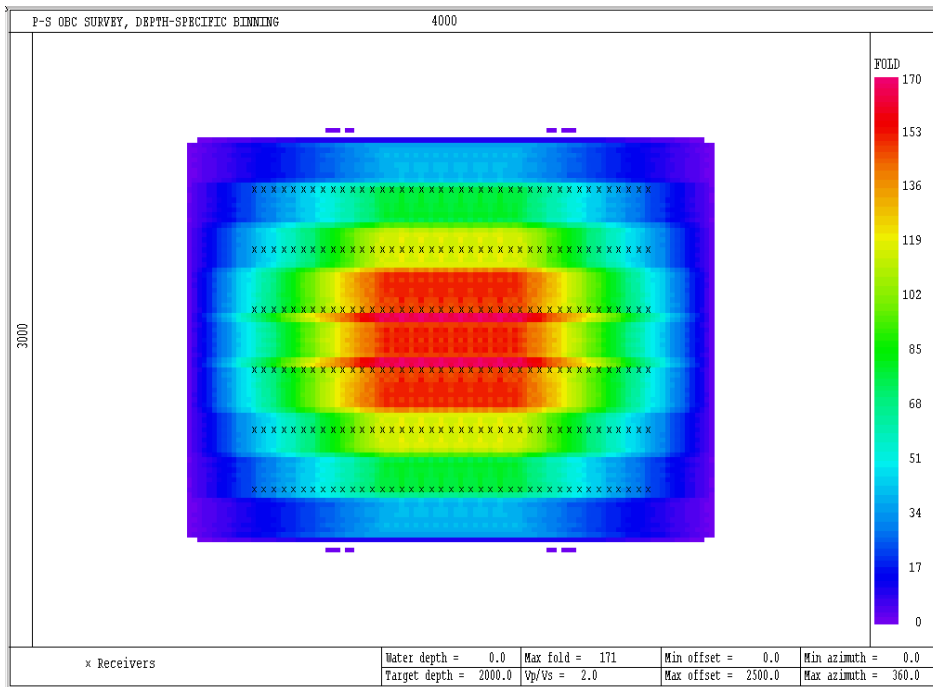


Figure 10. Depth-specific conversion point (DSCP) P-S fold for a target depth at 2000m and $V_p/V_s = 2.0$. Sinc-function interpolation applied.

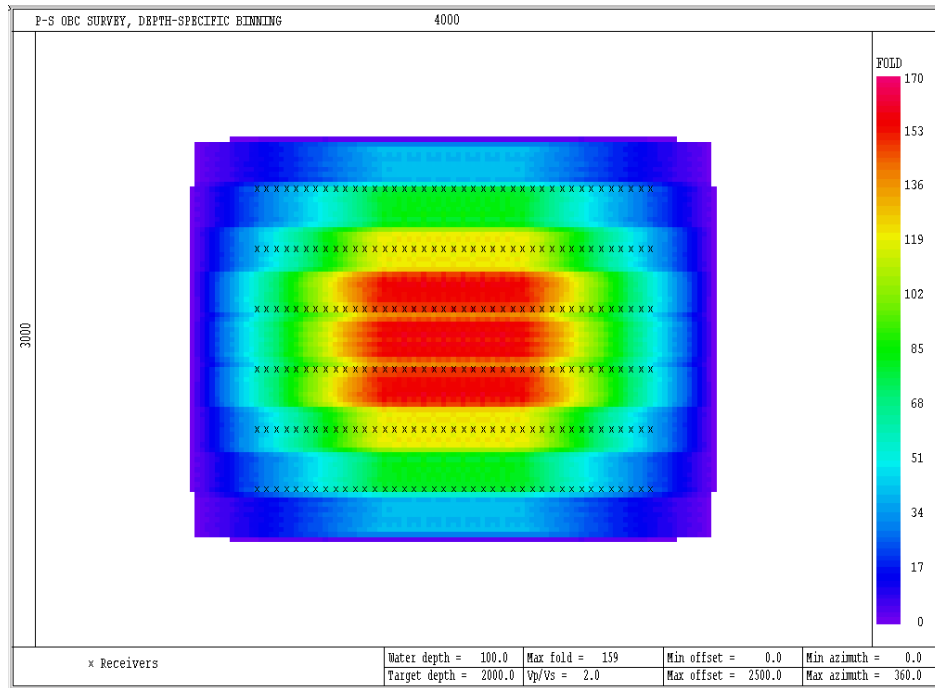


Figure 11. Depth-specific conversion point (DSCP) P-S fold for $V_p/V_s = 2.0$, target depth = 2000 m and receiver depth = 100 m. Sinc-function interpolation applied.

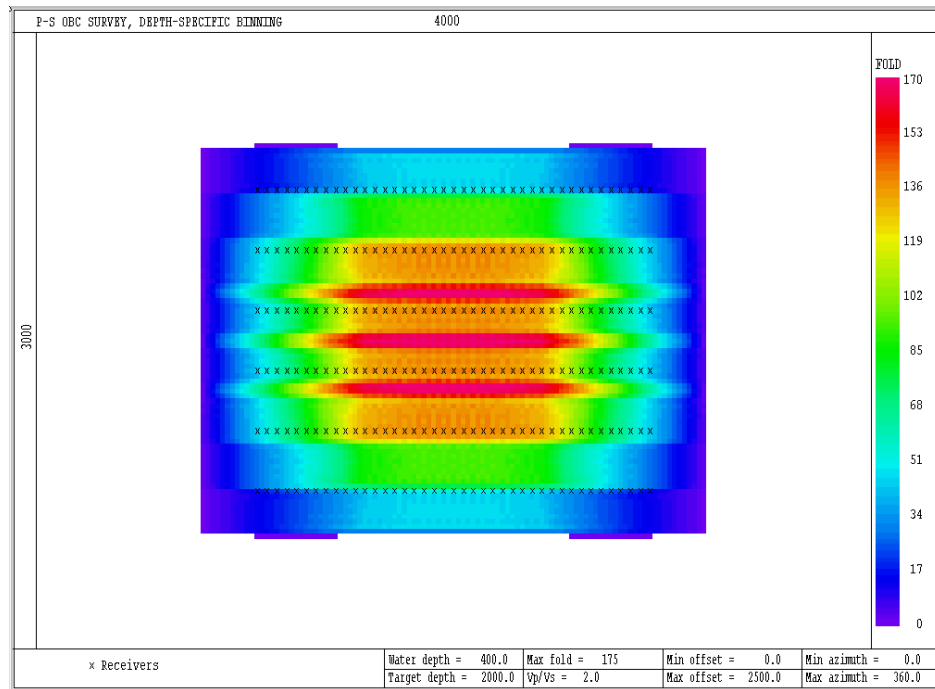


Figure 12. Depth-specific conversion point (DSCP) P-S fold for $V_p/V_s = 2.0$, target depth = 2000 m and receiver depth = 400 m. Sinc-function interpolation applied.

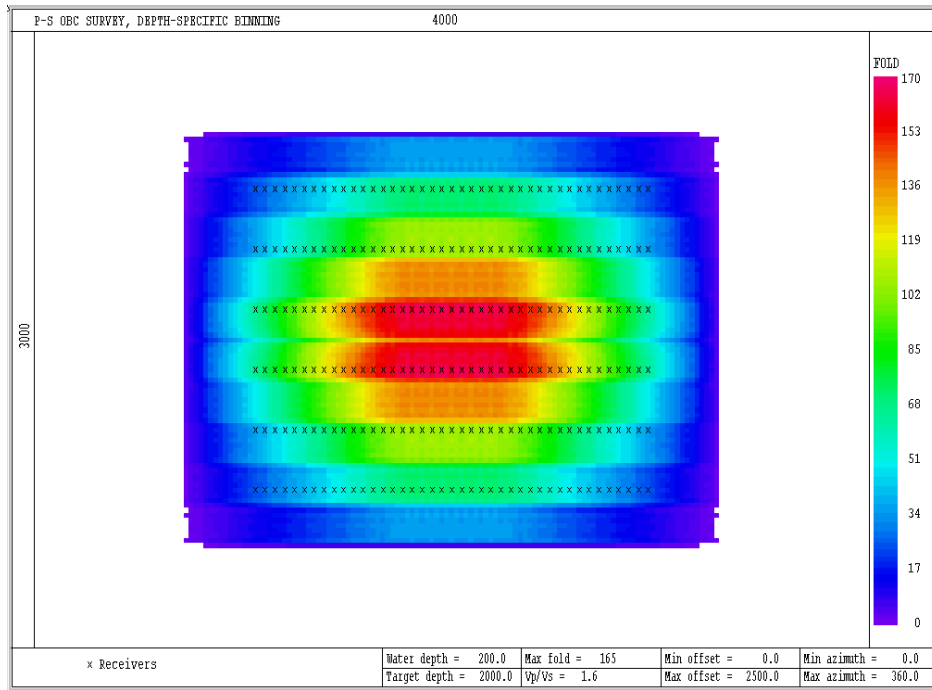


Figure 13. Depth-specific conversion point (DSCP) P-S fold for $V_p/V_s = 1.6$, target depth = 2000 m and receiver depth = 200 m. Sinc-function interpolation applied.

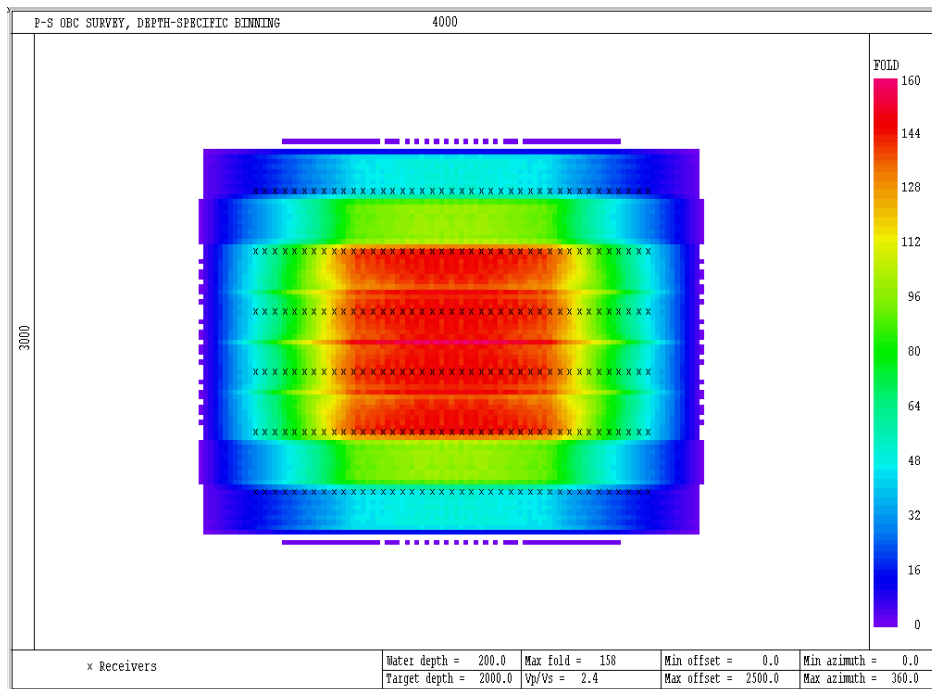


Figure 14. Depth-specific conversion point (DSCP) P-S fold for $V_p/V_s = 2.4$, target depth = 2000 m and receiver depth = 200 m. Sinc-function interpolation applied.